DOI: 10.1002/cmdc.200800341

Synthesis, Chiral Resolution and Pharmacological Evaluation of a 2,3-Benzodiazepine-Derived Noncompetitive AMPA Receptor Antagonist

Maria Luisa Calabrò,[a] Daniela Raneri,[a] Paola Ficarra,[a] Tiziana Mennini,[b] Simona Colleoni,[b] Giovanni Grazioso,[c] Nicola Micale,*[a] Maria Zappalà,[a] and Silvana Grasso[a]

*The resolution of 1-(4-aminophenyl)-3,5-dihydro-3-N-ethylcarbamoyl-5-methyl-7,8-methylenedioxy-4*H*-2,3-benzodiazepin-4-one (*R,S*)-(±)-**5** by chiral HPLC and assignment of the absolute configuration of the two enantiomers was carried out. Compound (*R,S*)-(±)-**5** and its enantiomers were tested in a binding assay to evaluate their affinity for AMPA receptors. Enantiomer (*S*)-(−)-**5** appears to be more potent than its optical antipode (*R*)-(+)-**5**. In a primary culture of rat cerebellar granule cells, which express AMPA receptors, (*R,S*)-(±)-**5** and (*S*)-(−)-**5** inhibited kainate-induced $[Ca^{2+}]_i$ increase, thus confirming the antagonism at the AMPA receptor.*

Introduction

α-Amino-3-hydroxy-5-methyl-4-isoxazole propionate receptors (AMPARs) are a group of glutamate-gated ion channels that are implicated as causative in the pathogenesis of numerous acute and chronic neurological disorders such as Parkinson's and Alzheimer's diseases, and epilepsy. Therefore, the identification and development of selective AMPARs ligands could have many potential therapeutic utilities.

Functional AMPARs are tetrameric structures, generated by the assembly of one or more distinct subunits defined GluR1–4. AMPAR subunits share a modular design consisting of an extracellular N-terminal domain, an extracellular agonist-binding domain formed by two segments (S1 and S2), an intracellular C-terminal trafficking and anchoring domain, a channel-forming domain consisting of three transmembrane domains (M1, M3 and M4), and a re-entrant loop (M2).[1]

There are a number of pharmacological agents that affect AMPAR function through interactions outside of the agonist-binding domain.[2] Among them are the 2,3-benzodiazepines; these are noncompetitive AMPAR antagonists whose prototype, 1-(4-aminophenyl)-4-methyl-7,8-methylenedioxy-5*H*-2,3-benzodiazepine (**1**, GYKI 52466) (Figure 1), demonstrated significant anticonvulsant and neuroprotective properties. These antagonists bind at the interface between the S1 and S2 glutamate-binding core and channel transmembrane domains, specifically interacting with S1–M1 and S2–M4 linkers, thereby disrupting the transduction of agonist binding into the channel opening.[1]

Highly active analogues of GYKI 52466 (**1**) have been identified, such as 3,4-dihydro-3-*N*-methylcarbamoyl [(±)-**2**, GYKI 53655] and 3,4-dihydro-3-*N*-acetyl [(±)-**3**, GYKI 53405] derivatives (Figure 1).[3] Both enantiomers of (±)-**2** and (±)-**3** have been evaluated and the eutomers turned out to be the (*R*)-enantiomer.[4] Subsequently, the eutomer (*R*)-(+)-**3** was chosen as a drug candidate and is now under clinical investigation as an anticonvulsant agent (LY 300164, Talampanel).[5] Recently, we

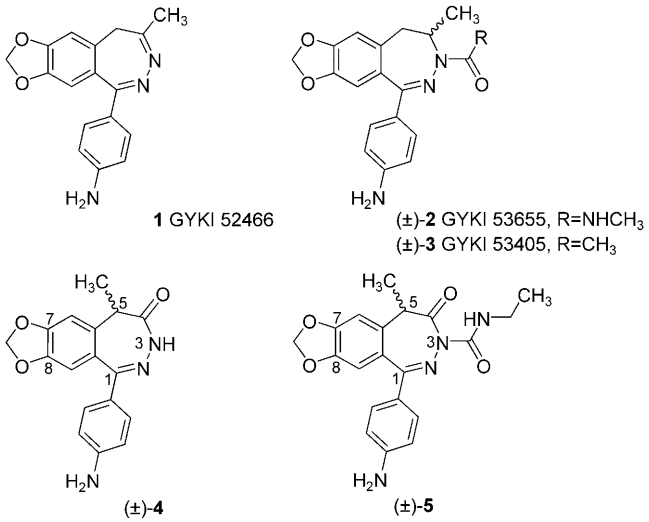

Figure 1. Structures of the 2,3-benzodiazepine derivatives **1**–**5**.

synthesized (±)-**4** (1-(4-aminophenyl)-3,5-dihydro-5-methyl-7,8-methylenedioxy-4*H*-2,3-benzodiazepin-4-one, see Figure 1) and conducted pharmacological assays that demonstrated an enantioselective interaction of the (*S*)-(−)-**4** enantiomer with

[a] *Prof. M. L. Calabrò, Dr. D. Raneri, Prof. P. Ficarra, Dr. N. Micale, Prof. M. Zappalà, Prof. S. Grasso*
Dipartimento Farmaco Chimico, University of Messina
Via le Annunziata, 98168, Messina (Italy)
Fax: (+39) 090 6766402
E-mail: nmicale@pharma.unime.it

[b] *Dr. T. Mennini, Dr. S. Colleoni*
Istituto di Ricerche Farmacologiche "Mario Negri"
Via La Masa 19, 20156 Milano (Italy)

[c] *Dr. G. Grazioso*
Istituto di Chimica Farmaceutica e Tossicologica "Pietro Pratesi"
University of Milano, Via Mangiagalli 25, 20133 Milano (Italy)

the noncompetitive binding site of the AMPARs. Notably, the configuration of (*S*)-(−)-**4** is inverted compared with that of Talampanel. However, a superimposition of the most populated conformation of the two molecules reveals extensive overlap of the common functional groups.[6]

In view of these interesting results, and considering the positive effect of the N-3 substituent in the GYKI 52466 analogues, we synthesized (±)-**5** (1-(4-aminophenyl)-3,5-dihydro-3-*N*-ethylcarbamoyl-5-methyl-7,8-methylenedioxy-4*H*-2,3-benzodiazepin-4-one, see Figure 1). The individual enantiomers were isolated by chiral HPLC and their absolute configuration assigned by computational methods. To evaluate the AMPAR affinity, racemate (±)-**5** and the pure enantiomers (+)-**5** and (−)-**5** were examined for their ability to displace [^{3}H]CP-526,427 from the noncompetitive binding site of the AMPARs, and the results were compared with those previously reported for the N-3 unsubstituted derivative **4**.

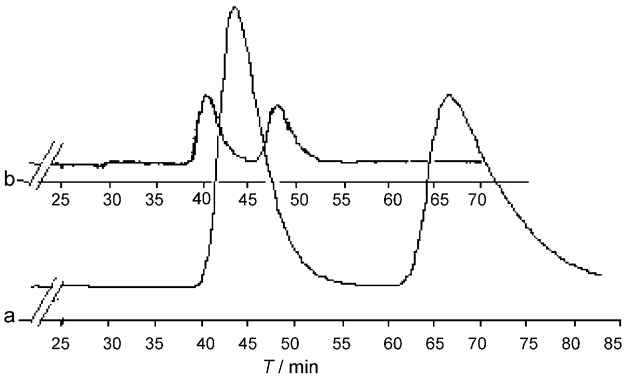

Figure 2. Enantiomeric resolution of (*R,S*)-(±)-**5** on Chiralcel OD (250×10 mm i.d., 10 μm) column at the concentrations of a) 2 mg mL^{-1} (250×4.6 mm i.d., 10 μm) and b) 0.48 mg mL^{-1}. For chromatographic conditions see text.

Results and Discussion

Synthesis

The synthesis of (*R,S*)-(±)-**5** was accomplished according to a procedure previously reported.[7] The treatment of compound **6** with ethyl isocyanate and subsequent Pd-catalyzed reduction gave (*R,S*)-(±)-**5** in good yields (Scheme 1).

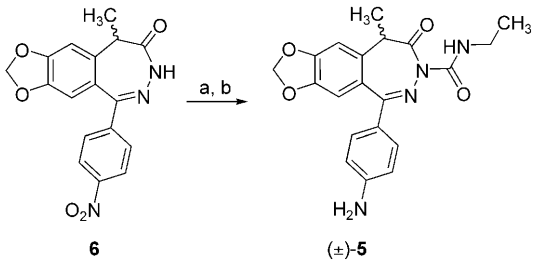

6 (±)-5

Scheme 1. The synthesis of (*R,S*)-(±)-**5**. *Reagents and conditions*: a) C_2H_5NCO, CH_2Cl_2, Et_3N, RT, 24 h; b) H_2, 5% Pd-C, $CHCl_3$, RT, 3 h, 62.5% overall.

Chiral HPLC analysis

A CSP-mobile phase optimization on a semipreparative scale was performed to isolate ~10 mg of each enantiomer for the investigation of the physical, structural and biological properties.

Enantiomeric resolution was performed by repetitive injections of 2 mg mL^{-1} of the sample on a 10 mm (ID) Chiralcel OD column. The results of enantioseparation of (*R,S*)-(±)-**5** are shown in Figure 2. Baseline resolution was obtained ($\alpha = 1.55$, $R_s = 2.03$) and retention times and resolutions were found to be stable for all the injections. The enantiomeric excess of the two fractions collected was monitored by analytical HPLC on a 4.6 mm (ID) Chiralcel OD column. Specific rotation of the first eluted enantiomer measured by polarimetric analysis was $[\alpha]_D^{20} = -215.2$ ($c = 0.42$, chloroform; *ee* 93.7%), while the second eluted enantiomer gave an experimental value of $[\alpha]_D^{20} = +149.36$ ($c = 0.47$, chloroform; *ee* 84.7%).

The analytical chiral method was validated in order to perform the optical purity assays on the two enantiomers.[8] Specificity of the quantitative analysis was given by the separation to baseline of the two enantiomers ($\alpha = 1.21$; $R_s = 1.69$). The range used to quantify the undesired enantiomer in a purity assay was 0.08–0.48 mg mL^{-1}. A calibration curve for both enantiomers was obtained from triplicate analyses at five different concentrations (0.08, 0.16, 0.32, 0.4, 0.48 mg mL^{-1}), and average values of the peak areas were subjected to linear regression analysis. Under the experimental conditions, linear relationships were found between the peak area and the enantiomer concentration (Figure 3).

To assess sensitivity of the assay, the limits of detection (LOD) and quantification (LOQ) were calculated from the standard deviation of the blank compared with the slope of the calibration curve, according to ICH Guideline. The calculated values for the LOD and LOQ were 3.51 and 10.63 μg mL^{-1}, respectively.

The accuracy and repeatability of the assay were established from replicate analyses across the specified concentration range. Each of the five compound concentrations was analyzed in triplicate. Accuracy was assessed as quantitative recovery percentage; the relative standard deviation (RSD) was calculated at each concentration to assess the repeatability. The results, reported in Table 1, showed that values obtained were in agreement with accepted validation procedures.

Assignment of the absolute configurations

To assign the absolute configuration of each enantiomer of compound (*R,S*)-(±)-**5**, several attempts were made to isolate crystals suitable for single crystal X-ray analysis. Since this approach failed, methodology based on the comparison of the experimental and the calculated $[\alpha]_D^{20}$ values was used. Examples of assignment of the absolute configuration in conformationally flexible molecules has been reported in the literature,[9]

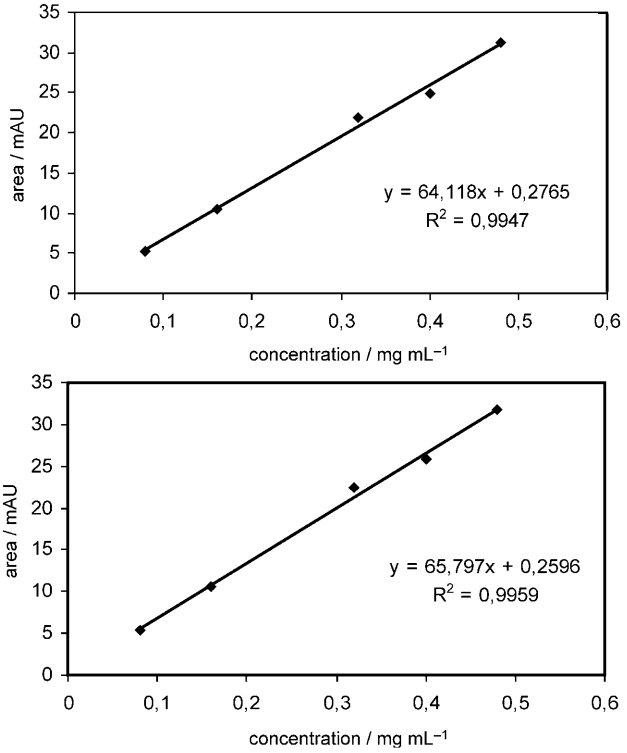

Figure 3. Linearity of the method for the determination of the enantiomers of (*R,S*)-(±)-**5.** a) first-eluting enantiomer (*S*)-(−)-**5**, b) second-eluting enantiomer (*R*)-(+)-**5**.

Table 1. Accuracy and repeatability of the proposed chiral HPLC method for the two enantiomers.[a]

Concentration	Recovery (%)		Intra-assay RSD (%)	
	(*S*)-(−)-**5**	(*R*)-(+)-**5**	(*S*)-(−)-**5**	(*R*)-(+)-**5**
0.08	98.82	97.63	4.98	6.33
0.16	102.18	99.74	0.97	1.04
0.32	79.07	93.66	0.34	1.56
0.4	83.70	101.86	1.22	1.38
0.48	131.17	99.37	2.75	2.20
Average	98.99	98.45	2.05	2.50

[a] Each data is the average of three determinations.

and this approach has recently been successfully applied to compound (*R,S*)-(±)-**4**.[6]

The systematic conformational analysis of compound (*R*)-**5** confirms that the 5-methyl-4*H*-2,3-benzodiazepin-4-one ring exists at room temperature in two stable geometries depending on the orientation of the methyl group (equatorial vs. axial). Similarly, the rotation of the 4-aminophenyl moiety linked at position 1 of the seven-membered ring introduces further conformational freedom that was optimized using the same method as previously described for compound **4**.[6] Moreover, an internal H bond is expected between the carbonyl group of the benzodiazepine ring and the NH group of the 3-*N*-ethylcarbamoyl moiety of compound **5** reducing the conformational freedom (Figure 4). Conversely, three different geometries for each benzodiazepine ring conformer were obtained

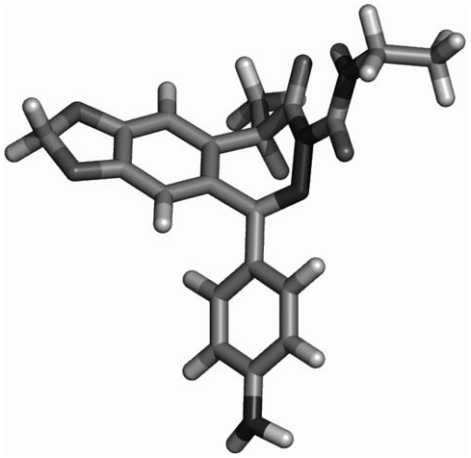

Figure 4. Three-dimensional plot of the global energy minimum conformation of compound (*R*)-**5** (conformer A) as optimized at the DFT/B3LYP/cc-pVTZ level using the PCM chloroform model. Figure was acquired by means of PYMOL software (DeLano, W. L. The PYMOL Molecular Graphics System (2002) DeLano Scientific, Palo Alto, CA, USA. http://www.pymol.org).

by rotating the torsion angle inner to the ethylcarbamoyl chain.

Five significantly populated spatial arrangements were found to hold the lowest energy potential at room temperature. The calculated $[\alpha]_D^{20}$ values of the diverse spatial arrangements of (*R*)-**5** were weight averaged to give an $[\alpha]_D^{20}$ value of +210.89, in good agreement with the experimental result of +149.36 (Table 2). As a consequence, the *R* configuration was assigned to (+)-**5**, which elutes second by HPLC.

Table 2. Calculated and experimental specific rotation of the different (*R*)-**5** enantiomer conformations.

Conformer	Population	E_{rel} [kcal mol^{-1}]	$[\alpha]_D^{20}$
(*R*)-**5 A**	41%	0.00	+241.12
(*R*)-**5 B**	33%	0.12	+230.05
(*R*)-**5 C**	24%	0.31	+168.50
(*R*)-**5 D**	1%	2.29	−216.00
(*R*)-**5 E**	1%	2.26	−327.24
Population weighed specific rotation			+210.89
Experimental optical specific rotation		First-eluted	−215.20
		Second-eluted	+149.36

Pharmacology

Racemic (*R,S*)-(±)-**5** and the pure enantiomers (*R*)-(+)-**5** and (*S*)-(−)-**5** were examined for their ability to displace [^{3}H]CP-526,427 from the noncompetitive 2,3-benzodiazepine binding site of the AMPAR complex (Table 3, Figure 5). In this assay, the quinazolinone CP-465,022 was used as a positive control (IC_{50} = 25 nM).[7] Compounds (*R,S*)-(±)-**5** and (*S*)-(−)-**5** showed IC_{50} values of 56.8 and 33.6 μM, respectively; whereas enantiomer (*R*)-(+)-**5** did not displace [^{3}H]CP-526,427 to any significant extent up to 300 μM. However, the eutomer (*S*)-(−)-**5** is approximately tenfold less potent than the 3-unsubstituted

Table 3. Pharmacological data of compounds **1**, **4** and **5**.

Compound	[^{3}H]CP-526,427 IC_{50} [μM][a]	KA-[Ca^{2+}]$_i$ IC_{50} [μM][a]
1	12.6	22
(*R,S*)-(±)-**4**	12.9	12
(*S*)-(−)-**4**	3.27	6
(*R,S*)-(±)-**5**	56.8	7
(*S*)-(−)-**5**	33.6	5.7
(*R*)-(+)-**5**	>300	>32

[a] IC_{50} values are representative of three different experiments. Variability ≤10%.

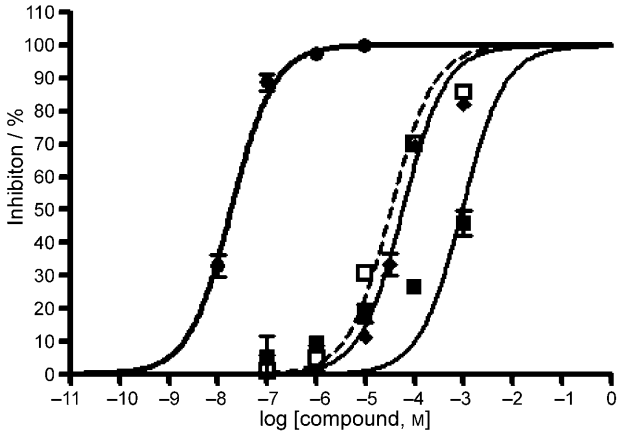

Figure 5. Inhibitory effects of (*R,S*)-(±)-**5** (◆) and its enantiomers ((−)-**5**, □; (+)-**5**, ■). Compounds were incubated at the indicated concentrations with rat forebrain membranes and 3 nM [^{3}H]CP-526,427 and bound radioactivity was determined. Nonspecific binding was determined for each point in parallel incubations containing 10 μM CP-465,022 (●) and specific binding was calculated as total minus nonspecifically bound radioactivity. Percent inhibition of [^{3}H]CP-526,427 binding was then calculated as: 100-[(Specific bound - nonspecific bound)/specific bound when no added compound) x100]. Each point is the mean ±SEM of 3–4 experiments, carried out in triplicate.

analogue (*S*)-(−)-**4** (IC_{50} = 3.27 μM)[6] and threefold less potent than lead compound **1** (IC_{50} = 12.6 μM)[7] in this assay.

Racemate (*R,S*)-(±)-**5** and the pure enantiomers were also tested for their inhibition of functional AMPAR-mediated responses; namely, kainate-induced $^{45}Ca^{2+}$ uptake in a primary culture of rat cerebellar granule cells expressing AMPARs.[10] Compound **1** was used as the control in the assay. Compound (*R,S*)-(±)-**5** and the eutomer (*S*)-(−)-**5** produced an almost complete inhibition of the calcium influx at 32 μM with IC_{50} values of 7 and 5.7 μM, respectively. These values are comparable to that of compound (*S*)-(−)-**4** (IC_{50} = 6 μM)[6] and better than that reported for compound **1** (IC_{50} = 22 μM),[11] thus confirming the AMPAR antagonism (Table 3).

Notably, the configuration of the eutomer of both compounds **4** and **5** is (*S*)-(−), which is opposite to that of Talampanel, (*R*)-(+)-**3**. Since the noncompetitive binding site of the AMPARs has yet to be characterized by X-ray analysis, we performed a superimposition of (*R*)-(+)-**3** (Talampanel) and the most populated conformations of both enantiomers of compound **5** (Figure 6). This comparison reveals significant overlap

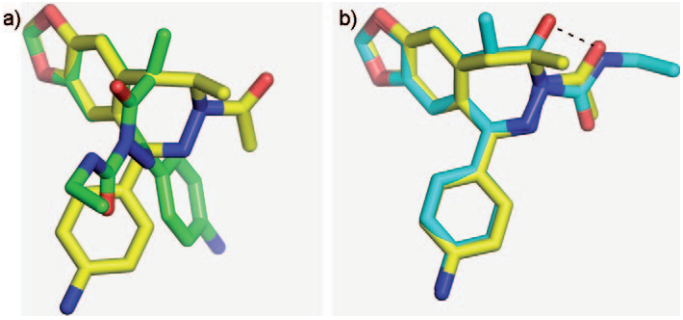

Figure 6. Superimposition of Talampanel [(*R*)-(+)-**3**] (yellow) with a) (*R*)-(+)-**5** (green) or b) (*S*)-(−)-**5** (cyan).

of both the aromatic portions for the eutomer (*S*)-(−)-**5** with (*R*)-(+)-**3**, along with a short distance (2,36 Å) between the carbonyl group at C-4 of (*S*)-(−)-**5** and the side chain of (*R*)-(+)-**3**. Conversely, there is less overlap between these essential pharmacophoric groups for (*R*)-(+)-**5** with (*R*)-(+)-**3**, mainly because of the aminophenyl ring at C-1. Furthermore, a different orientation of the alkyl group connected to the carbamoyl chain of (*S*)-(−)-**5** with respect to the side chain alkyl group of (*R*)-(+)-**3** was found. This chain has reduced conformational freedom due to the H-bond between the carbonyl group of the benzodiazepine ring and the NH of the 3-*N*-ethylcarbamoyl moiety.

Most likely, the *N*-ethyl group could create steric hindrance in the binding site leading to a weaker biological activity. Such steric effects could also explain the lower AMPAR affinity of (*S*)-(−)-**5** compared with the affinity observed with the 3-unsubstituted derivative (*S*)-(−)-**4**.

Conclusions

In summary, the individual enantiomers of (*R,S*)-(±)-**5** have been isolated by chiral HPLC and their absolute configuration assigned by a comparison of the experimental and the calculated specific rotation values. The pharmacological assays indicated an enantioselective interaction of the enantiomer (*S*)-(−)-**5** with the noncompetitive binding site of the AMPARs. This result has been rationalized through the overlapping of its most populated conformation with the structure of Talampanel [(*R*)-(+)-**3**], a known ligand of the AMPAR noncompetitive binding site.

Experimental Section

Synthesis

Melting points were determined on a Kofler hot stage apparatus and are uncorrected. Elemental analyses were carried out on a Carlo Erba Elemental Analyzer for C, H and N (Model 1106) and the results are within ±0.4% of the theoretical values. Merck silica gel 60 F_{254} plates were used for analytical TLC; column chromatography was performed on Merck silica gel 60 (70–230 mesh). ^{1}H NMR spectra were recorded in $CDCl_3$ using a Varian Gemini 300 Hz spectrometer. Chemical shifts are expressed in δ (ppm) relative to TMS as an internal standard, and coupling constants (*J*) are given in Hz.

Synthesis of 1-(4-aminophenyl)-3,5-dihydro-3-*N*-ethylcarbamoyl-5-methyl-7,8-methylenedioxy-4*H*-2,3-benzodiazepin-4-one (±)-5: A solution of compound **6**[6] (300 mg, 0.88 mmol) in CH_2Cl_2 (50 mL) was treated with TEA (1.15 mL, 8.23 mmol) and ethyl isocyanate (0.36 mL, 4.42 mmol) and stirred at RT for 24 h. The reaction mixture was washed with 5% HCl, then saturated NaCl solution, and extracted with $CHCl_3$. The organic phase was dried (Na_2SO_4), filtered and concentrated in vacuo. The resulting residue was purified by trituration with Et_2O and used without further purification. Catalytic hydrogenation was carried out at atmospheric pressure. A solution of the crude nitro derivative (350 mg) in $CHCl_3$ (50 mL) was treated with 5% Pd-C (50 mg) and the mixture was shaken under H_2 for 3 h. The catalyst was removed by filtration through a Celite pad and the filtrate was washed with H_2O and saturated NaCl solution, the aqueous phase was then extracted with $CHCl_3$. The combined organic layers were dried (Na_2SO_4), filtered and concentrated in vacuo. The crude residue was purified by column chromatography ($CHCl_3$/EtOAc, 50:50) to afford (±)-**5** as a white solid, which was further purified by trituration with Et_2O. Mp: 120–123 °C (210 mg, 62.5%); $R_f = 0.61$ (EtOAc/*c*-C_6H_{12}, 80:20); ^{1}H NMR (300 MHz, $CDCl_3$): $\delta = 1.18$ (t, 3H, $J = 7.1$ Hz, CH_3CH_2), 1.56 (d, 3H, $J = 6.9$ Hz, CH_3-5), 3.22–3.40 (m, 2H, CH_2CH_3), 3.49 (q, 1H, $J = 6.9$ Hz, CH), 3.97 (br s, 2H, NH_2), 6.02–6.06 (m, 2H, OCH_2O), 6.68 (d, 2H, $J =$ 8.5 Hz, H-3′,5′), 6.73 (s, 1H, H-9), 6.87 (s, 1H, H-6), 7.58 (d, 2H, $J =$ 8.5 Hz, H-2′,6′), 8.78 (t, 1H, NH) ppm; Anal. calcd for $C_{20}H_{20}N_4O_4$: C 63.15, H 5.30, N 14.73, found: C 63.39, H 5.13, N 14.53.

Chiral HPLC analysis

HPLC grade 2-propanol and ethanol were purchased from Merck (Darmstadt, Germany). All solutions employed in the separations were filtered through 0.45 μm Sartorius Minisart® SRP 15 PTFE filters (Hanover, Germany). The enantiomers were isolated by semipreparative chiral HPLC, by means of a Shimadzu LC-10 AD VP system pump, equipped with a Rheodyne model 7125–075 injector with a 200 μL sample loop. Normal phase chromatography was carried out on a semipreparative cellulose *tris*-3,5-dimethylphenylcarbamate column (Chiralcel OD, 250×10 mm (ID), 10 μm, Daicel Chemical, Tokyo, Japan), at 20 °C, with a mobile phase of *n*-hexane/2-propanol (80:20) and a flow rate of 4.8 mL min^{-1}. A Shimadzu SPD-10 A VP detector was used and chromatograms were processed with Shimadzu CLASS VP CDS 4.3. In order to perform the chiral purity assays for both enantiomeric fractions, an analytical chiral HPLC method was carried out and validated. The analyses were performed on a Perkin–Elmer series 410 liquid chromatograph, equipped with a septumless injector (Rheodyne 7125–075) with a 6 μL sample loop. The stationary phase used was an analytical chiral column (Chiralcel OD, 250×4.6 mm (ID), 10 μm, Daicel Chemical, Tokyo, Japan), thermostated at 20 °C with a column heater (Perkin–Elmer TC 931). A variable wavelength diode array detector (Perkin–Elmer LC 235) was used. Peak area integration was performed using a chromatographic data system (Perkin–Elmer LCI 100 laboratory computing integrator). The mobile phase was *n*-hexane/2-propanol/ethanol (78:19:3) with a flow rate of 0.85 mL min^{-1}. The detector wavelength was set at 235 nm either for both the semipreparative and the analytical methods. All solutions investigated in the separation were filtered through 0.45 μm PTFE Minisart SRP 15 filters provided by Sartorius (Hanover, Germany). The stability of the solutions at 20 °C was checked by HPLC analysis every third day for 2 months, no racemization was observed. Optical rotations were measured in chloroform on a polarimeter (Perkin–Elmer model 341) equipped with a sodium lamp, at a wavelength of 589 nm. The volume of the measuring cell was 1 mL and the optical path length was 10 cm. The system was thermostated at 20 °C.

Assignment of the absolute configurations

The absolute configuration of compound **5** was assigned by comparing the experimental and the calculated $[\alpha]_D^{20}$ values of the (*R*)-enantiomer. The molecular structures were built by means of GaussView software implemented in the Gaussian 03 package.[12] Following the computational procedure recently described for compound **4**,[6] we built the two minimal conformational geometries of the benzodiazepine ring related to the enantiomer (*R*)-**5**. Then, taking into account the results of a potential energy scan performed on the ethylcarbamoyl moiety at the AM1 theory level, three different geometries of this external chain were combined to the previously built benzodiazepine ring conformers. The resultant structures were optimized at the b3lyp/6–31 g* level and the conformer population was calculated by optimizing the PCM chloroform solvent model at the DFT/B3LYP/cc-pVTZ theory level. The theoretical $[\alpha]_D^{20}$ values were calculated from a single point calculation for each conformer.

[^{3}H]CP-526,427 binding

The binding of [^{3}H]CP-526,427 was performed in rat forebrain membranes.[10] Forebrains of adult male Sprague-Dawley rats (Charles River, Calco, Como, Italy) were homogenized in 0.32 M sucrose at 4 °C. The crude nuclear pellet was removed by centrifugation at 1,000 *g* for 10 min, and the supernatant centrifuged at 17,000 *g* for 25 min. The resulting pellet was re-suspended in 5 mM Tris acetate, pH 7.4, at 4 °C for 10 min to lyse cellular particles and again centrifuged at 17,000 *g*. The resulting pellet was washed twice in Tris acetate, re-suspended at 10 mg of protein mL^{-1} and stored at −20 °C until use. Immediately before binding assays were conducted, membranes were thawed, homogenized, and diluted to 0.5 mg of protein mL^{-1} with 50 mM Tris·HCl, pH 7.4. For competition assays, compounds were added at various concentrations followed by 3 nM [^{3}H]CP-526,427 (specific activity, 24.36 Ci mmol^{-1}). After incubation for 20 min at 30 °C in a shaking water bath, samples were filtered through Whatman GFB glass fiber filters using a MB-48R Cell Harvester (Brandel Research and Development Laboratories, Gaithersburg MD). Filters were washed with ice-cold Tris·HCl buffer and the radioactivity trapped on the filter quantified by Tri-Carb 2800 TR liquid scintillation β-counter (PerkinElmer). Nonspecific binding for [^{3}H]CP-526,427 was determined in parallel samples containing unlabeled CP-465,022 (10 μM). The inhibitory effects observed in the different experiments were pooled together and the inhibition curves were analyzed using the "one site competition" equation built into GraphPad Prism 4.0 (GraphPad Software, San Diego, CA) to give the associated IC_{50} values (i.e. the compound concentration inhibiting specific binding by 50%).

Inhibition of kainate-induced increase of the $[Ca^{2+}]_i$

These experiments were carried out in primary cultures of rat cerebellar granule neurons according to the method previously described.[10,13]

Procedures involving animals and their care were conducted in conformity with the institutional guidelines that are in compliance with national (D.L. n.116 G.U., suppl. 40, 1992 Feb. 18) and international (EEC Council Directive 86/609, OJ L 358, 1, 1987 Dec. 12;

Guide for the Care and Use of Laboratory Animals, US National Research Council, 1996) laws and policies.

Acknowledgements

We would like to thank Dr. F. S. Menniti*, Pfizer Global Research and Development, Groton, Connecticut (USA) for supplying us with the [^{3}H]CP-526,427 radioligand.*

Keywords: 2,3-benzodiazepin-4-one · absolute configuration · ampar · binding assays · chiral HPLC

[1] V. Balannik, F. S. Menniti, A. V. Paternain, J. Lerma, Y. Stern-Bach, *Neuron* **2005**, *48*, 279–288.
[2] J. N. Kew, J. A. Kemp, *Psychopharmacology* **2005**, *179*, 4–29.
[3] T. Szabados, G. Gigler, I. Gacsályi, I. Gyertán, G. Lévay, *Brain Res. Bull.* **2001**, 55, 387–391.
[4] S. Sólyom, I. Tarnawa, *Curr. Pharm. Des.* **2002**, *8*, 913–939.
[5] A. S. Chappell, J. W. Sander, M. J. Brodie, D. Chadwick, A. Lledo, D. Zhang, J. Bjerke, G. M. Kiesler, S. Arroyo, *Neurology* **2002**, *58*, 1680–1682.
[6] M. Zappalà, G. Postorino, N. Micale, S. Caccamese, N. Parrinello, G. Grazioso, G. Roda, F. S. Menniti, G. Ferreri, G. De Sarro, S. Grasso, *J. Med. Chem.* **2006**, *49*, 575–581.
[7] N. Micale, S. Colleoni, G. Postorino, A. Pellicanò, M. Zappalà, J. T. Lazzaro, V. Diana, A. Cagnotto, T. Mennini, S. Grasso, *Bioorg. Med. Chem.* **2008**, *16*, 2200–2211.
[8] International Conference on Harmonisation of Technical Requirements for Registration of Pharmaceuticals for Human Use (ICH), ICH Harmonised Tripartite Guideline, Validation of Analytical Procedures: Text and Methodology Q2(R1), available online at http://www.ich.org/LOB/media/MEDIA417.pdf.
[9] a) P. J. Stephens, F. J. Devlin, J. R. Cheeseman, M. J. Frisch, C. Rosini, *Org. Lett.* **2002**, *4*, 4595–4598; b) B. Mennucci, J. Tomasi, R. Cammi, J. R. Cheeseman, M. J. Frisch, F. J. Devlin, S. Gabriel, P. J. Stephens, *J. Phys. Chem. A* **2002**, *106*, 6102–6113; c) E. Giorgio, M. Roje, K. Tanaka, Z. Hamersak, V. Sunjic, K. Nakanishi, C. Rosini, N. Berova, *J. Org. Chem.* **2005**, *70*, 6557–6563; d) A. C. Petrovic, J. He, P. L. Polavarapu, L. S. Xiao, D. W. Armstrong, *Org. Biomol. Chem.* **2005**, *3*, 1977–1981.
[10] F. S. Menniti, B. L Chenard, M. B. Collins, M. F. Ducat, M. L. Elliot, F. E. Ewing, J. I. Huang, K. A. Kelly, J. T. Lazzaro, M. J. Pagnozzi, J. L. Weeks, W. M. Welch, W. F. White, *Mol. Pharmacol.* **2000**, *58*, 1310–1317.
[11] M. Zappalà, A. Pellicanò, N. Micale, F. S. Menniti, G. Ferreri, G. De Sarro, S. Grasso, C. De Micheli, *Bioorg. Med. Chem. Lett.* **2006**, *16*, 167–170.
[12] Gaussian 03, Revision C.02, M. J. Frisch, G. W. Trucks, H. B. Schlegel, G. E. Scuseria, M. A. Robb, J. R. Cheeseman, Jr., J. A. Montgomery, T. Vreven, K. N. Kudin, J. C. Burant, J. M. Millam, S. S. Iyengar, J. Tomasi, V. Barone, B. Mennucci, M. Cossi, G. Scalmani, N. Rega, G. A. Petersson, H. Nakatsuji, et al. Gaussian, Inc., Wallingford CT, **2004**.
[13] T. N. Parks, L. D. Artman, N. Alasti, E .F. Nemeth, *Brain Res.* **1991**, *552*, 13–22.

Received: October 15, 2008
Revised: November 11, 2008
Published online on January 9, 2009

